

Figure 2 | Untitled 5 and its box-counting curve. The best broken power-law fit to these data corresponds to slopes of $D_D = 1.53$ and $D_I = 1.84$. The break occurs at $\ln(L) \approx 4$; the standard deviation of the data from the fit, χ_2 is 0.022. *Untitled 5* (top) fulfils all the criteria used in box-counting authentication that have been made public: it shows a broken power-law behaviour with $D_D < D_I$ and, for a magnification factor C similar to that used by Taylor *et al.*, has a χ_2 value in the 'permissible' range of $0.009 < \chi < 0.025$. **Methods.** All our sketches, including *Untitled 5*, are freehand drawings made in Adobe Photoshop using a 14-point Adobe Photoshop 'paintbrush'. The paintbrush leaves a mark when dragged continuously across the 'canvas' by a computer mouse. Although not drip paintings, these patterns are human- and not computer-generated, in the sense that these terms are commonly understood and as used by Taylor *et al.*⁴. The box sizes were chosen to be hC^n , where $n = 1, 2, 3, \dots, M$. Here $h = 3$ pixels is the smallest box size, the magnification factor $C = 1.12$, the cutoff M determines the biggest box size, and the box sizes range over about 1.9 orders of magnitude.

drip paintings (out of about 180). Further study of systematic effects is needed. As the values measured by Taylor *et al.*⁹ are not available, a consensus on the limiting range, if there is one, can emerge only after other groups have replicated and extended the box-counting data set. Finally, we note that *Untitled 5* fulfils all the criteria used in box-counting authentication that have so far been made public.

Katherine Jones-Smith, Harsh Mathur

Department of Physics, Case Western Reserve

University, Cleveland, Ohio 44106, USA

e-mail: hxm7@case.edu

1. Abbott, A. *Nature* **439**, 648–650 (2006).
2. Taylor, R. P., Micolich, A. P. & Jonas, D. *Nature* **399**, 422 (1999).
3. Taylor, R. P., Micolich, A. P. & Jonas, D. *Phys. World* **12**, 25–28 (1999).
4. Taylor, R. P., Micolich, A. P. & Jonas, D. *Leonardo* **35**, 203–207 (2002).
5. Taylor, R. P. in *Art and Complexity* (eds Casti, J. & Karlqvist, A.) 117–144 (Elsevier, Amsterdam, 2003).
6. Mandelbrot, B. B. *The Fractal Geometry of Nature* (Freeman, New York, 1977).

7. Avnir, D., Biham, O., Lidar, D. & Malcai, O. *Science* **279**, 39–40 (1998).
8. Mandelbrot, B. B. *Science* **279**, 783 (1998).
9. Taylor, R. P. *et al. Patt. Recog. Lett.* (in the press) (materialsscience.uoregon.edu/taylor/art/TaylorPRL.pdf).
10. Namuth, H. & Falkenberg, P. *Jackson Pollock* (Collectors Series film, The Museum of Modern Art, New York, 1950).
11. Landau, E. G. *Jackson Pollock* (Thames and Hudson, London, 1989).
12. Ott, E. *Chaos in Dynamical Systems* (Cambridge University Press, Cambridge, 2002).
13. Mureika, J. R., Cupchik, G. C. & Dyer, C. C. *Leonardo* **37**, 53–56 (2004).

doi:10.1038/nature05398

FRactal ANALYSIS

Taylor et al. reply

Replying to: K. Jones-Smith & H. Mathur *Nature* 444, doi:10.1038/nature05398

Our use¹ of the term 'fractal'² is consistent with that by the research community. In dismissing Pollock's fractals^{1,3} because of their limited magnification range, Jones-Smith and Mathur⁴ would also dismiss half the published investigations of physical fractals⁵. On the basis of previous debates on limited-range fractals^{5,6}, a fractal description is particularly appropriate for Pollock's patterns because it is physically reasonable and because it is useful for condensing the description of a complex geometry, as we now describe.

Fractal description is physically reasonable because Pollock's technique involved a motion-dominated process at large length scales and a paint-dominated process at small scales, with a transition between the two expected at several centimetres. The fractal behaviours observed in the scaling plots above and below this transition are physically reasonable — many physiological processes⁷, including human motion^{8,9}, are fractal, and falling liquid can itself be fractal¹⁰.

However, for *Untitled 5* there is no physical reason to expect a transition between two processes at $\ln(L) \approx 4$. In the absence of this artificial transition, the scaling plot does not fit fractal behaviour. Furthermore, when we generate 'drawings' similar to *Untitled 5*, some plots curve down and some curve up (Fig. 1a), in contrast to the consistent behaviour observed in Pollock's poured paintings. Combined, these observations demonstrate that the "freehand sketches" of Jones-Smith and Mathur⁴ are not fractal. Hence, *Untitled 5* does not undermine any claim that we have made about Pollock's work.

As to the usefulness of a fractal description, Pollock's fractals satisfy all the criteria for usefulness proposed for limited-range fractals⁵. Furthermore, our fractal description of Pollock's patterns is useful across disciplines, for example in psychology experiments (showing that Pollock's fractals induce the same perceptual responses as mathematical fractals¹¹), and

in applications of fractal geometry to distinguish paintings by different artists^{3,12}.

We disagree with the claim by Jones-Smith and Mathur⁴ that Pollock's fractal characteristics are easily generated by gaussian random motion. Our simulations generate scaling plots with variable curvature (Fig. 1b), in contrast to the consistent behaviour shown in Pollock's paintings¹².

It is both mathematically and physically possible for two exposed patterns and their composite all to be fractal. This depends on the relative densities of the exposed patterns and the scaling behaviour of boxes containing both patterns. Jones-Smith and Mathur's Cantor dust does not apply to Pollock paintings, where the overlap of layers is considerably more complicated. Furthermore, their Fig. 1a features box counts of less than one (in reality, a box is either filled or not). The gradient of their green trace becomes greater than one (impossible for an object with $0 < D < 1$). Their Fig. 1a also misleads because it concentrates on large scales — the deviation of the blue and composite box counts becomes insignificant at finer scales (Fig. 1c).

We performed an actual box count on the dust analysed by Jones-Smith and Mathur (Fig. 1d) in order to show that their analytical simulations are flawed. Their expressions are evaluated at each iteration, instead of correctly box counting after fully generating the pattern. Their green curve is generated by using an expression that holds only for specific cases in which a 'box' exactly matches the width of a Cantor dust segment: it is therefore invalid for most of the continuous range the authors display.

Finally, we keep the value of the magnification factor C constant in recent authenticity procedures because χ_2 is dependent on C (ref. 12, which also gives our authenticity criteria, which are not confidential). We encourage further research.

R. P. Taylor*, **A. P. Micolich†**, **D. Jonas‡**

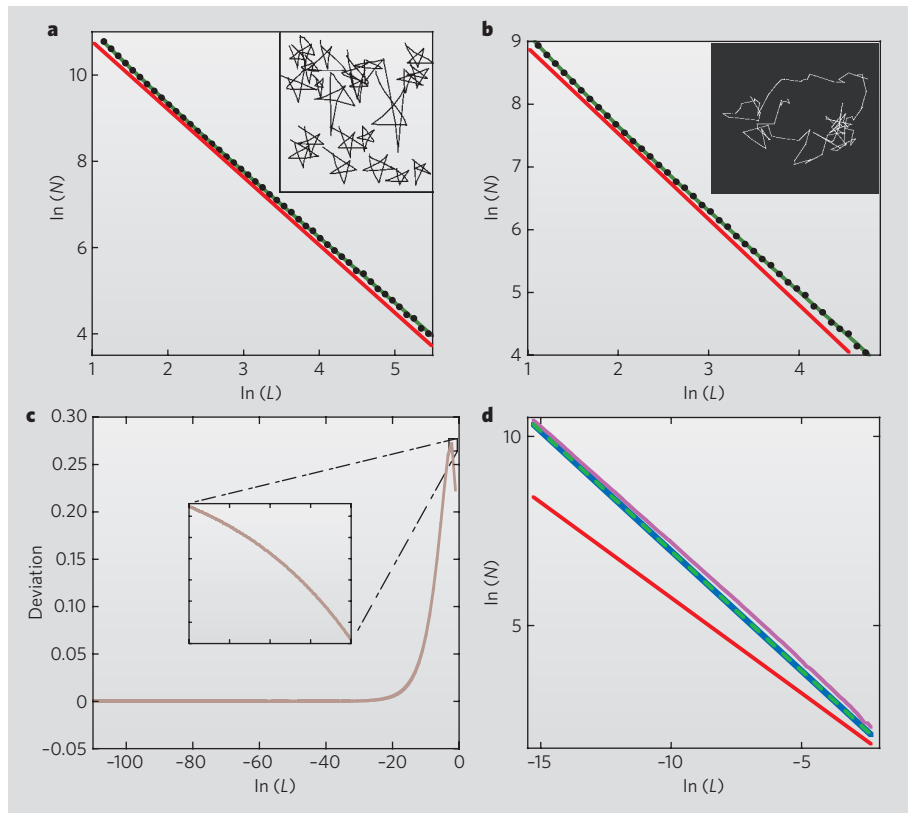


Figure 1 | Analysis of freehand, gaussian and Cantor dust patterns. **a, b**, Example images (insets) and scaling plots of **a**, 'freehand' and **b**, gaussian patterns. Both plots deviate from the scaling behaviour found in Pollock's paintings. **c**, Brown trace from Fig. 1a of Jones-Smith and Mathur⁴, plotted over a large scaling range and showing that the deviation is insignificant over most of the graph. Inset, limited region selected by Jones-Smith and Mathur⁴. **d**, A standard box count performed on the Cantor dust of ref. 4 (see their Fig. 1a for colour coding). In contrast to their analytical simulations, our green trace is rigorously linear over six orders of magnitude, deviating from the blue trace only when the box size matches the dust's finest features. T. P. Martin, B. C. Scannell and M. S. Fairbanks contributed to this analysis.

Methods. For **a, b**, the 'freehand sketch' and gaussian random walk were generated as in Jones-Smith and Mathur⁴. Green lines are third-order polynomial fits to the data; red lines act as a guide to the eye, illustrating the data's upward curvature. For **c**, we iterate the analytical expression of Jones-Smith and Mathur⁴ to produce our brown curve. For **d**, we generate their Cantor dust to seven iterations to ensure appropriate statistics and then perform a standard box counting. To ensure sufficient counting statistics, the largest box size plotted corresponds to one-tenth of the image.

*Physics Department, University of Oregon,
Eugene, Oregon 97403, USA

e-mail: rpt@uoregon.edu

†School of Physics, University of New South
Wales, Sydney, New South Wales 2052, Australia

1. Taylor, R. P., Micolich, A. P. & Jonas, D. *Nature* **399**, 422 (1999).
2. Mandelbrot, B. B. *The Fractal Geometry of Nature* (Freeman, New York, 1977).
3. Mureika, J. R., Dyer, C. C. & Cupchik, G. C. *Phys. Rev. E* **72**, 046101-1-15 (2005).
4. Jones-Smith, K. & Mathur, H. *Nature*

doi:10.1038/nature05398 (2006).

5. Avnir, D., Biham, O., Lidar, D. & Malcai, O. *Science* **279**, 39-40 (1998).
6. Mandelbrot, B. B. *Science* **279**, 783 (1998).
7. Bassingthwaite, J. B., Liebovitch, L. S. & West, B. J. *Fractal Physiology* (Oxford Univ. Press, 1994).
8. Hausdorff, J. M. et al. *J. Appl. Physiol.* **80**, 1448-1457 (1996).
9. Doyle, T. et al. *Int. J. Med. Sci.* **1**, 11-20 (2004).
10. Shi, X. D. et al. *Science* **265**, 219-222 (1994).
11. Aks, D. & Sprott, J. C. *Empir. Stud. Arts* **14**, 1-16 (1996).
12. Taylor, R. P. et al. *Patt. Recog. Lett.* (in the press).

doi:10.1038/nature05399